Available online at www.sciencedirect.com
ScienceDirect
Physics Letters B 641 (2006) 440–446
PHYSICS LETTERS B
www.elsevier.com/locate/physletb

Hadron optics: Diffraction patterns in deeply virtual Compton scattering

S.J. Brodsky [a], D. Chakrabarti [b], A. Harindranath [c], A. Mukherjee [d,*], J.P. Vary [e,a,f]

[a] Stanford Linear Accelerator Center, Stanford University, Stanford, CA 94309, USA
[b] Department of Physics, University of Florida, Gainesville, FL 32611-8440, USA
[c] Saha Institute of Nuclear Physics, 1/AF Bidhannagar, Kolkata 700064, India
[d] Department of Physics, Indian Institute of Technology, Powai, Mumbai 400076, India
[e] Department of Physics and Astronomy, Iowa State University, Ames, IA 50011, USA
[f] Lawrence Livermore National Laboratory, L-414, 7000 East Avenue, Livermore, CA 94551, USA

Received 3 May 2006; received in revised form 9 August 2006; accepted 25 August 2006

Available online 12 September 2006

Editor: N. Glover

Abstract

We show that the Fourier transform of the deeply virtual Compton scattering (DVCS) amplitude with respect to the skewness variable ζ at fixed invariant momentum transfer squared t provides a unique way to visualize the structure of the target hadron in the boost-invariant longitudinal coordinate space. The results are analogous to the diffractive scattering of a wave in optics. As a specific example, we utilize the quantum fluctuations of a fermion state at one loop in QED to obtain the behavior of the DVCS amplitude for electron–photon scattering. We then simulate the wavefunctions for a hadron by differentiating the above LFWFs with respect to M^2 and study the corresponding DVCS amplitudes in light-front longitudinal space. In both cases we observe that the diffractive patterns in the longitudinal variable conjugate to ζ sharpen and the positions of the first minima move in with increasing momentum transfer. For fixed t, higher minima appear at positions which are integral multiples of the lowest minimum. Both these observations strongly support the analogy with diffraction in optics.

1. Introduction

Deeply virtual Compton scattering (DVCS) $\gamma^*(q) + p(P) \to \gamma(q') + p(P')$ provides a remarkable tool for studying the fundamental structure of the proton at the amplitude level. We define the momentum transfer $\Delta = P - P'$ and the invariant momentum transfer squared $t = \Delta^\mu \Delta_\mu$. When the incoming photon is highly virtual $Q^2 = -q^2 \gg \Lambda^2_{\rm QCD}$, the underlying scattering process measures Compton scattering on bound quarks, convoluted with the fundamental microscopic wavefunctions of the initial- and final-state proton. In addition, the initial-state photon can scatter on virtual $q\bar{q}$ pairs in the target which are then annihilated by the final-state photon, thus probing the particle-number quantum fluctuations of the hadron wavefunction required for Lorentz invariance. Measurements of the DVCS cross sections with specific proton and photon polarizations can provide comprehensive probes of the spin as well as spatial structure of the proton at the most fundamental level of QCD.

The theoretical analysis of DVCS is particularly clear and compelling when one utilizes light-front quantization at fixed $\tau = y^+$. (We use the standard LF coordinates $P^\pm = P^0 \pm P^3$, $y^\pm = y^0 \pm y^3$. Since the proton is on-shell, $P^+P^- - P^2_\perp = M^2_p$.) If we neglect radiative corrections to the struck quark propagator (i.e., set the Wilson line to 1), then the required DVCS quark matrix elements can be computed from the overlap of the boost-invariant light-front Fock state wavefunctions (LFWFs) of the target hadron [1,2]. The longitudinal momentum transfer to the target hadron is given by the "skewness" variable $\zeta = \frac{Q^2}{2p\cdot q}$. Since the incoming photon is space-like ($q^2 < 0$) and the final photon is on-shell ($(q')^2 = 0$), the skewness is never zero in a physical experiment. The DVCS process involves off-forward hadronic matrix elements of light-front

* Corresponding author.
E-mail address: asmita@phy.iitb.ac.in (A. Mukherjee).

doi:10.1016/j.physletb.2006.08.061

bilocal currents. Accordingly, in different kinematical regions, there is a diagonal parton-number conserving $n \to n$ overlap and an off-diagonal $n+1 \to n-1$ overlap where the parton number is decreased by two. Thus, given the LFWFs one then obtains a complete specification of all of the generalized parton distributions (GPDs) measurable in DVCS, including their phase structure. The sum rules of DVCS, such as Ji's sum rule for angular momentum [3] and the integral relations to electromagnetic and gravitational form factors are all explicitly satisfied in the light-front (LF) formalism [1,2].

In this Letter we shall show how one can use measurements of the dependence of the DVCS amplitude on the skewness variable ζ to obtain a novel optical image of a hadron target, in analogy to the way in which one scatters optical waves to form a diffraction pattern. In this context, it is useful to introduce a coordinate b conjugate to the momentum transfer Δ such that $b \cdot \Delta = \frac{1}{2} b^+ \Delta^- + \frac{1}{2} b^- \Delta^+ - b_\perp \cdot \Delta_\perp$. Note that $\frac{1}{2} b^- \Delta^+ = \frac{1}{2} b^- P^+ \zeta = \sigma \zeta$ where we have defined the boost invariant variable σ which is an 'impact parameter' in the longitudinal coordinate space. The Fourier transform of the DVCS amplitude with respect to ζ allows one to determine the longitudinal structure of the target hadron in terms of the variable σ.

Burkardt [4,5] has studied the off-forward parton distribution function at zero longitudinal momentum transfer and fixed longitudinal momentum fraction x in the impact parameter $(b_\perp)$ space. This relativistic impact representation on the light-front was introduced earlier by Soper [6] in the context of the Fourier transform of the elastic form factor. We study the DVCS amplitude, which involves integration over x, in the σ space at fixed four-momentum transfer $-t$. Note that experimentally DVCS amplitudes are measured as a function of ζ and $-t$. Thus, our work is suited for the direct analysis of experimental data and is complementary to the work of Burkardt and Soper. If one combines the longitudinal transform (at fixed $\Delta_\perp$) with the Fourier transform (FT) of the DVCS amplitude with respect to $\Delta_\perp$ one can obtain a complete three-dimensional description of hadron optics at fixed LF time.

Recently, a 3D picture of the proton has been proposed in [7] in a different approach, in terms of a Wigner distribution for the relativistic quarks and gluons inside the proton. A major difference of this from our work is that the Wigner distributions are defined in the rest frame of the proton. Integrating out k^- one gets the reduced Wigner distributions which are not observable quantities in the quantum domain. Further integration over $k^\perp$ relates them to the FT of GPDs $H(x,\xi,t)$ and $E(x,\xi,t)$, where $\xi = q^z/2E_q$ and x is a special combination of off shell energy and momentum along z. On the other hand, we are taking the FT of the experimentally measurable DVCS amplitudes directly and not the GPDs.

In principle, the LFWFs of hadrons in QCD can be computed using a non-perturbative method such as discretized light cone quantization (DLCQ) where the LF Hamiltonian is diagonalized on a free Fock basis [8]. This has been accomplished for simpler confining quantum field theories such as QCD(1 + 1) [9]. Models for the LFWFs of hadrons in (3 + 1) dimensions displaying confinement at large distances and conformal symmetry at short distances have been obtained using the AdS/CFT method [10]. The light front longitudinal space structure of topological objects has been studied in DLCQ [11].

In order to illustrate our general framework, we will present here an explicit calculation of the σ transform of virtual Compton scattering on the quantum fluctuations of a lepton in QED at one-loop order [12], the same system which gives the Schwinger anomalous moment $\alpha/2\pi$. This model has the advantage that it is Lorentz invariant, and thus it has the correct relationship between the diagonal $n \to n$ and the off-diagonal $n-1 \to n+1$ Fock state contributions to the DVCS amplitude. One can generalize this analysis by assigning a mass M to the external electrons and a different mass m to the internal electron lines and a mass λ to the internal photon lines with $M < m + \lambda$ for stability. In effect, we shall represent a spin-$\frac{1}{2}$ system as a composite of a spin-$\frac{1}{2}$ fermion and a spin-1 vector boson [13–15]. We also will present numerical results for a composite hadron by taking a derivative of the LFWFs with respect to the hadron's mass M^2. This simulates the behavior of a bound-state hadron by improving the fall-off at the end points of the longitudinal momentum fraction x. The summary of our main results will be given in this Letter. A more detailed analysis will be given in a forthcoming article [16].

2. DVCS in the LF formalism

The kinematics of the DVCS process has been given in detail in [1,2]. One can work in a frame where the momenta of the initial and final proton has a $\Delta \to -\Delta$ symmetry [2]. However, in this frame, the kinematics in terms of the parton momenta becomes more complicated. Here, we choose the frame of Ref. [1].

The virtual Compton amplitude $M^{\mu\nu}(\vec{q}_\perp, \vec{\Delta}_\perp, \zeta)$, i.e., the transition matrix element of the process $\gamma^*(q) + p(P) \to \gamma(q') + p(P')$, can be defined from the light-cone time-ordered product of currents

$$M^{\mu\nu}(\vec{q}_\perp, \vec{\Delta}_\perp, \zeta) = i \int d^4 y \, e^{-iq\cdot y} \langle P' | T J^\mu(y) J^\nu(0) | P \rangle, \quad (1)$$

where the Lorentz indices μ and ν denote the polarizations of the initial and final photons, respectively. In the limit $Q^2 \to \infty$ at fixed ζ and t the Compton amplitude is thus given by

$$\begin{aligned} &M^{IJ}(\vec{q}_\perp, \vec{\Delta}_\perp, \zeta) \\ &\quad = \epsilon^I_\mu \epsilon^{*J}_\nu M^{\mu\nu}(\vec{q}_\perp, \vec{\Delta}_\perp, \zeta) \\ &\quad = -e_q^2 \frac{1}{2\bar{P}^+} \int_{\zeta-1}^{1} dz \bigg\{ t^{IJ}(z,\zeta) \bar{U}(P') \bigg[H(z,\zeta,t)\gamma^+ \\ &\qquad + E(z,\zeta,t) \frac{i}{2M} \sigma^{+\alpha}(-\Delta_\alpha) \bigg] U(P) \bigg\}, \end{aligned} \quad (2)$$

where $\bar{P} = \frac{1}{2}(P' + P)$ and we take a frame in which $q^+ = 0$. For DVCS, when Q^2 is large compared to the masses and $-t$, we have,

$$\frac{Q^2}{2P \cdot q} = \zeta \quad (3)$$

up to corrections in $1/Q^2$. Thus ζ plays the role of the Bjorken variable in deeply virtual Compton scattering. For a fixed value of $-t$, the allowed range of ζ is given by

$$0 \leqslant \zeta \leqslant \frac{(-t)}{2M^2}\left(\sqrt{1+\frac{4M^2}{(-t)}}-1\right). \tag{4}$$

For simplicity we only consider one quark with flavor q and electric charge e_q. We here consider the contribution of only the spin-independent GPDs H and E. Throughout our analysis we will use the "handbag" approximation where corrections to the hard quark propagator are neglected.

For circularly polarized initial and final photons (I, J are $\uparrow$ or $\downarrow$) contributions only come from

$$t^{\uparrow\uparrow}(z,\zeta) = t^{\downarrow\downarrow}(z,\zeta) = \frac{1}{z-i\epsilon} + \frac{1}{z-\zeta+i\epsilon}. \tag{5}$$

For a longitudinally polarized initial photon, the Compton amplitude is of order $1/Q$ and thus vanishes in the limit $Q^2 \to \infty$. At order $1/Q$ there are several corrections to the simple structure in Eq. (2). We do not consider them here.

The generalized parton distributions H, E are defined through matrix elements of the bilinear vector and axial vector currents on the light-cone:

$$\begin{aligned} &F_{\lambda,\lambda'}(z,t) \\ &\quad= \int \frac{dy^-}{8\pi} e^{izP^+y^-/2} \langle P',\lambda'|\bar\psi(0)\gamma^+\psi(y)|P,\lambda\rangle|_{y^+=0,y_\perp=0} \\ &\quad= \frac{1}{2\bar P^+}\bar U(P',\lambda') \\ &\qquad\times\left[H(z,\zeta,t)\gamma^+ + E(z,\zeta,t)\frac{i}{2M}\sigma^{+\alpha}(-\Delta_\alpha)\right] \\ &\qquad\times U(P,\lambda). \end{aligned} \tag{6}$$

The off-forward matrix elements given by Eq. (6) can be expressed in terms of overlaps of LFWFs of the state [1,2]. For this, we take the state to be an electron in QED at one loop and consider the LFWFs for this system.

The light-front Fock state wavefunctions corresponding to the quantum fluctuations of a physical electron can be systematically evaluated in QED perturbation theory. The state is expanded in Fock space and there are contributions from $|e^-\gamma\rangle$ and $|e^-e^-e^+\rangle$, in addition to renormalizing the one-electron state. The two-particle state is expanded as,

$$\begin{aligned} &\left|\Psi^\uparrow_{\text{two particle}}(P^+,\vec P_\perp=\vec 0_\perp)\right\rangle \\ &\quad= \int \frac{dx\, d^2\vec k_\perp}{\sqrt{x(1-x)}16\pi^3} \\ &\qquad\times\Big[\psi^\uparrow_{+\frac12+1}(x,\vec k_\perp)\left|+\tfrac12+1;xP^+,\vec k_\perp\right\rangle \\ &\qquad+\psi^\uparrow_{+\frac12-1}(x,\vec k_\perp)\left|+\tfrac12-1;xP^+,\vec k_\perp\right\rangle \\ &\qquad+\psi^\uparrow_{-\frac12+1}(x,\vec k_\perp)\left|-\tfrac12+1;xP^+,\vec k_\perp\right\rangle \\ &\qquad+\psi^\uparrow_{-\frac12-1}(x,\vec k_\perp)\left|-\tfrac12-1;xP^+,\vec k_\perp\right\rangle\Big], \end{aligned} \tag{7}$$

where the two-particle states $|s^z_{\rm f}, s^z_{\rm b}; x, \vec k_\perp\rangle$ are normalized as in [1]. The variables $s^z_{\rm f}$ and $s^z_{\rm b}$ denote the projection of the spins of the constituent fermion and boson along the quantization axis, and the variables x and $\vec k_\perp$ refer to the momentum of the fermion. The light cone momentum fractions $x_i = \frac{k_i^+}{P^+}$ satisfy $0 < x_i \leqslant 1$, $\sum_i x_i = 1$. We employ the light-cone gauge $A^+ = 0$, so that the gauge boson polarizations are physical. The three-particle state has a similar expansion. Both the two- and three-particle Fock state components are given in [1]. We list here the two-particle wavefunctions for the spin-up electron [1,12,17]

$$\begin{cases} \psi^\uparrow_{+\frac12+1}(x,\vec k_\perp) = -\sqrt2\frac{-k^1+ik^2}{x(1-x)}\varphi, \\ \psi^\uparrow_{+\frac12-1}(x,\vec k_\perp) = -\sqrt2\frac{k^1+ik^2}{1-x}\varphi, \\ \psi^\uparrow_{-\frac12+1}(x,\vec k_\perp) = -\sqrt2(M-\frac{m}{x})\varphi, \\ \psi^\uparrow_{-\frac12-1}(x,\vec k_\perp) = 0, \end{cases} \tag{8}$$

$$\varphi(x,\vec k_\perp) = \frac{e}{\sqrt{1-x}}\frac{1}{M^2 - \frac{\vec k_\perp^2+m^2}{x} - \frac{\vec k_\perp^2+\lambda^2}{1-x}}. \tag{9}$$

Similarly, the wavefunction for an electron with negative helicity can also be obtained.

In the domain $\zeta < z < 1$, there are diagonal $2 \to 2$ overlap contributions to Eq. (6), both helicity flip, F^{22}_{+-} ($\lambda' \neq \lambda$) and helicity non-flip, F^{22}_{++} ($\lambda' = \lambda$) [1]. The GPDs $H_{(2\to2)}(z,\zeta,t)$ and $E_{(2\to2)}(z,\zeta,t)$ are zero in the domain $\zeta - 1 < z < 0$, which corresponds to emission and re-absorption of an e^+ from a physical electron. Contributions to $H_{(n\to n)}(z,\zeta,t)$ and $E_{(n\to n)}(z,\zeta,t)$ in that domain only appear beyond one-loop level. This is because in the DVCS amplitude we have integrations over z, y^-, and x. When integration over y^- is performed, the fermion part of the bilocal current yields a factor $\delta(z-x)$ and the anti-fermion part of the bilocal current yields a factor $\delta(z+x)$. The latter contribution is absent in the one loop DVCS amplitude of a electron target, which we consider in the present work.

The matrix elements F^{22}_{++} and F^{22}_{+-} are calculated using the two-particle LFWFs given in Eq. (8). The contributions in the domain, $0 < z < \zeta$, namely, F^{31}_{+-} and F^{31}_{++} come from overlaps of three-particle and one-particle LFWFs [1]. These are calculated using the three-particle wavefunction. Explicit expressions of all the above matrix elements will be given in [16].

We calculate the DVCS amplitude given by Eq. (2) using the off-forward matrix elements calculated above. In order to regulate the ultraviolet divergences, we use a cutoff Λ on the transverse momentum $k^\perp$. The real and imaginary parts are calculated separately using the prescription

$$\begin{aligned} &\int_0^1 dx \frac{1}{x-\zeta+i\epsilon} F(x,\zeta) \\ &\quad= P\int_0^1 dx \frac{1}{x-\zeta}F(x,\zeta) - i\pi F(\zeta,\zeta). \end{aligned} \tag{10}$$

Here P denotes the principal value defined as

$$P\int_0^1 dx \frac{1}{x-\zeta} F(x,\zeta)$$

$$= \lim_{\epsilon\to 0}\left[\int_0^{\zeta-\epsilon} \frac{1}{x-\zeta} F(x,\zeta) + \int_{\zeta+\epsilon}^1 \frac{1}{x-\zeta} F(x,\zeta)\right], \qquad (11)$$

where

$$F(x,\zeta) = F_{ij}^{31}(x,\zeta,\Delta_\perp), \quad \text{for } 0<x<\zeta$$
$$= F_{ij}^{22}(x,\zeta,\Delta_\perp), \quad \text{for } \zeta<x<1$$

with $ij = ++$ for helicity non-flip and $ij = +-$ for helicity flip amplitudes. Since the off-forward matrix elements are continuous at $x=\zeta$, $F(\zeta,\zeta) = F_{ij}^{22}(x=\zeta,\zeta,\Delta_\perp) = F_{ij}^{31}(x=\zeta,\zeta,\Delta_\perp)$. Note that the principal value prescription cannot be used at $x=0$. We take a small cutoff at this point for the numerical calculation. The off-forward matrix elements F^{31} (which contribute in the kinematical region $0<x<\zeta$) vanish as $x\to 0$, as a result there is no logarithmic divergence at this point for nonzero ζ. But, we need to be careful here as when we consider the Fourier transform in σ space, ζ can go to zero and divergences from small x can occur from F^{22} which is finite and nonzero at $x,\zeta\to 0$.

The imaginary part of the amplitude when the electron helicity is not flipped is then given by

$$\mathrm{Im}[M_{++}](\zeta,\Delta_\perp) = \pi e^2 F_{++}^{22}(x=\zeta,\zeta,\Delta_\perp). \qquad (12)$$

A similar expression holds in the case when the electron helicity is flipped ($\mathrm{Im}[M_{+-}](\zeta,\Delta_\perp)$) in which F_{++} are replaced by F_{+-}. The helicity-flip DVCS amplitude is proportional to $(\Delta_1 - i\Delta_2)$ [16]. Without any loss of generality, the plots for these amplitudes are presented with $\Delta_2 = 0$. The imaginary part receives contributions at $x=\zeta$. The other regions of x contribute to the real part. It is to be emphasized that we are using the handbag approximation of the DVCS amplitude. Contributions from the Wilson lines are in general not zero, and they can give rise to new phase structures as seen in single-spin asymmetries [18].

The real part of the DVCS amplitude in our model is given by

$$\mathrm{Re}[M_{++}](\zeta,\Delta_\perp)$$
$$= -e^2\int_{\epsilon}^{\zeta-\epsilon_1} dx\, F_{++}^{31}(x,\zeta,\Delta_\perp)\left[\frac{1}{x}+\frac{1}{x-\zeta}\right]$$
$$- e^2\int_{\zeta+\epsilon_1}^{1-\epsilon} dx\, F_{++}^{22}(x,\zeta,\Delta_\perp)\left[\frac{1}{x}+\frac{1}{x-\zeta}\right]. \qquad (13)$$

A similar expression holds for the helicity flip DVCS amplitude. The cutoff dependence at $x=\zeta$ in the principal value prescription gets canceled explicitly and, as a result, the DVCS amplitude is independent of the cutoff ϵ_1.

3. Calculation of the σ Fourier transform

In order to obtain the DVCS amplitude in longitudinal coordinate space, we take a Fourier transform in ζ as,

$$A_{++}(\sigma,t) = \frac{1}{2\pi}\int_{\epsilon_2}^{1-\epsilon_2} d\zeta\, e^{i\sigma\zeta} M_{++}(\zeta,\Delta_\perp),$$
$$A_{+-}(\sigma,t) = \frac{1}{2\pi}\int_{\epsilon_2}^{1-\epsilon_2} d\zeta\, e^{i\sigma\zeta} M_{+-}(\zeta,\Delta_\perp), \qquad (14)$$

where $\sigma = \frac{1}{2}P^+b^-$ is the (boost invariant) longitudinal distance on the light-cone and the FTs are performed at a fixed invariant momentum transfer squared $-t$. We have imposed cutoffs at $\epsilon = \epsilon_1 = \epsilon_2/2 = 0.001$ for the numerical calculation.

A detailed discussion of the cutoff scheme will be given in [16].

All Fourier transforms (FT) have been performed by numerically calculating the Fourier sine and cosine transforms and then calculating the resultant by squaring them, adding and taking the square root, thereby yielding the Fourier spectrum (FS). In Fig. 1, we have shown the FS of the imaginary part of the DVCS amplitude for $M = 0.51$ MeV, $m = 0.5$ MeV and $\lambda = 0.02$ MeV. (a) is the helicity non-flip and (b) is the helicity flip part of the amplitude. We have divided the amplitude by the normalization constant $e^4/(16\pi^3)$ and have taken $\Lambda = Q = 10$ MeV. The helicity non-flip amplitude depends on the scale Λ logarithmically and the scale dependence is suppressed in the helicity-flip part. As seen in Fig. 1(a), the FS of the imaginary part of the helicity non-flip amplitude displays a diffraction pattern in σ. The peak initially increases with increasing $-t$, but then decreases as $-t$ increases further. The latter behavior warrants further study. In contrast, we see in Fig. 1(b) that there is no diffraction pattern in the FS of the imaginary part of the helicity flip amplitude. This is due to different behavior with respect to ζ of the respective amplitudes [16]. Further, note that in this case the peak monotonically increases with increasing $-t$. One reason for this may be the presence of the extra factor of $\Delta_\perp$ in the helicity flip amplitude compared to the helicity non-flip amplitude.

In Fig. 2 we have plotted the Fourier spectrum of the real part of the DVCS amplitude vs. σ for $M = 0.51$ MeV, $m = 0.5$ MeV and $\lambda = 0.02$ MeV. For the same $|t|$, the behavior is independent of Q when $|t| < m^2$. For each Q, the peak at $\sigma = 0$ is sharper and higher as $|t|$ increases, the number of minima within the same σ range also increases. As seen in Fig. 2, the FS of both the helicity flip and helicity non-flip parts show a diffraction pattern.

The DVCS amplitude for an electron-like state at one loop has potential singularities at $x = 1$. As mentioned above, we have used cutoffs at $x = 0, 1$. The cutoff at $x = 0$ is imposed for the numerical integration. In the 2- and 3-body LFWFs, the bound-state mass squared M^2 appears in the denominator. Differentiation of the LFWFs with respect to M^2 increases the fall-off of the wavefunctions near the end points $x = 0, 1$ and mimics the hadronic wavefunctions. In this way, the cut-

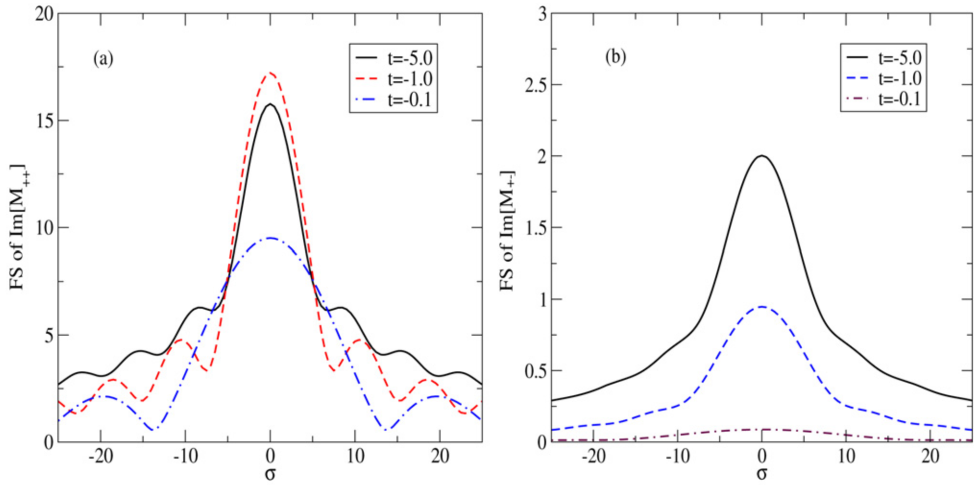

Fig. 1. Fourier spectrum of the imaginary part of the DVCS amplitude of an electron vs. σ for $M = 0.51$ MeV, $m = 0.5$ MeV, $\lambda = 0.02$ MeV, (a) when the electron helicity is not flipped; (b) when the helicity is flipped. The parameter t is in MeV^2.

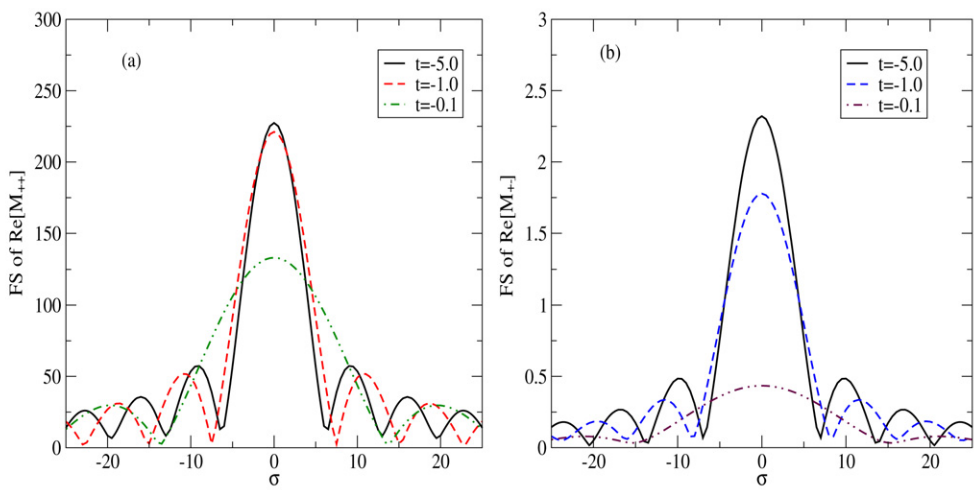

Fig. 2. Fourier spectrum of the real part of the DVCS amplitude of an electron vs. σ for $M = 0.51$ MeV, $m = 0.5$ MeV, $\lambda = 0.02$ MeV, (a) when the electron helicity is not flipped; (b) when the helicity is flipped. The parameter t is in MeV^2.

off dependency is removed. Differentiating once with respect to M^2 simulates a meson-like wavefunction and another differentiation simulates a proton wavefunction. Convolution of these wavefunctions in the same way as we have done for the dressed electron wavefunctions will simulate the corresponding DVCS amplitudes for bound state hadrons. One has to note that differentiation of the single particle wave function yields zero and thus there is no $3-1$ overlap contribution to the DVCS amplitude in this hadron model. It is to be noted that in recent holographic models from AdS/CFT as well [10], only valence LFWFs are constructed.

The equivalent but easier way is to differentiate the DVCS amplitude with respect to the initial and final state masses. Here we calculate the quantity $M_F^2 \frac{\partial}{\partial M_F^2} M_I^2 \frac{\partial}{\partial M_I^2} A_{ij}(M_I, M_F)$ where M_I, M_F are the initial and final bound state masses. For numerical computation, we use the discrete (in the sense that the denominator is small and finite but not limiting to zero) version of the differentiation

$$M^2 \frac{\partial A}{\partial M^2} = \bar{M}^2 \frac{A(M_1^2) - A(M_2^2)}{\delta M^2}, \tag{15}$$

where $\bar{M}^2 = \frac{(M_1^2 + M_2^2)}{2}$ and $\delta M^2 = (M_1^2 - M_2^2)$. We have taken $M_{I1}, M_{F1} = 150 + 1$, $M_{I2}, M_{F2} = 150 - 1$ MeV and fixed parameters $M = 150$ and $m = \lambda = 300$ MeV. In Figs. 3 and 4 we have shown the DVCS amplitude of the simulated hadron model, both as a function of ζ and after taking the FT in ζ. In Fig. 4(c), we have plotted the structure function $F_2(x)$ in this model. The wave function is normalized to 1. Recall that the $\gamma^* p \to \gamma p$ DVCS amplitude has both real [19] and imaginary parts [20]. The imaginary part requires a non-vanishing LFWF at $x' = \frac{x-\zeta}{1-\zeta} = 0$. If we consider a dressed electron, the imaginary part from the pole at $x = \zeta$ survives because of the numerator $\frac{1}{x-\zeta}$ factor in the electron's LFWF. This numerator behavior reflects the spin-1 nature of the constituent boson. The $x - \zeta \to 0$ singularity is shielded when we differentiate the final state LFWFs with respect to M^2 and, as a result, the imaginary part of the amplitude vanishes in this model. We thus have constructed a model where the DVCS amplitude is purely real. It is interesting that the forward virtual Compton amplitude $\gamma^* p \to \gamma^* p$ (whose imaginary part gives the structure function) does not have this property. The pole at $x = \zeta$ is

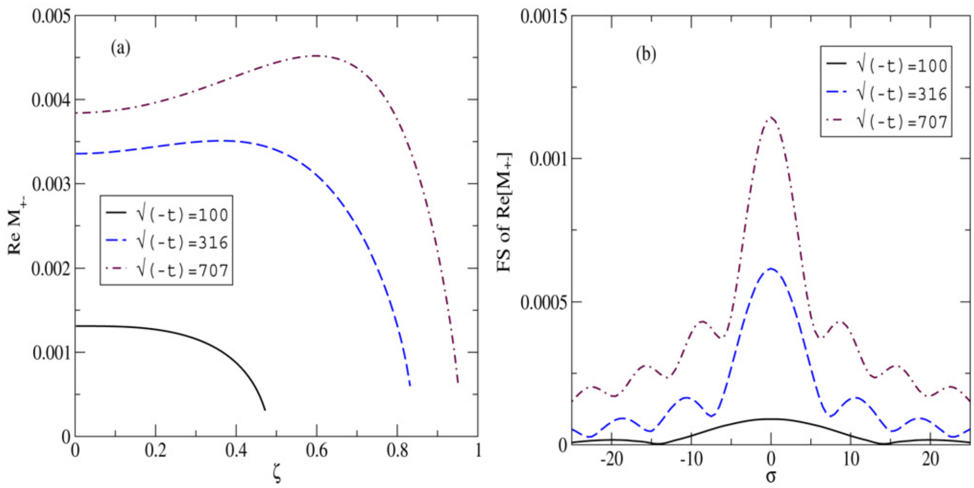

Fig. 3. Real part of the DVCS amplitude for the simulated meson-like bound state. The parameters are $M = 150$, $m = \lambda = 300$ MeV. (a) Helicity flip amplitude vs. ζ; (b) Fourier spectrum of the same vs. σ. The parameter t is in MeV^2.

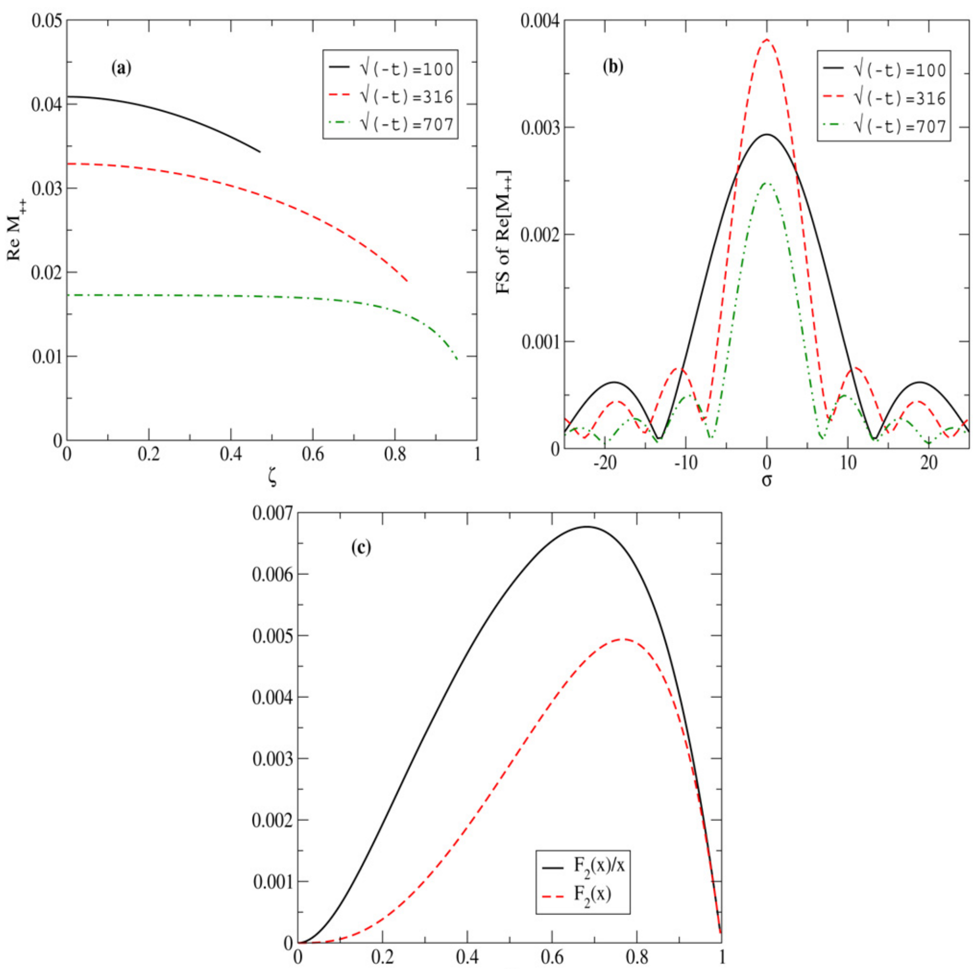

Fig. 4. Real part of the DVCS amplitude for the simulated meson-like bound state. The parameters are $M = 150$, $m = \lambda = 300$ MeV. (a) Helicity non-flip amplitude vs. ζ; (b) Fourier spectrum of the same vs. σ; (c) structure function vs. x. The parameter t is in MeV^2.

not shielded since the initial and final $n = 2$ LFWFs are functions of x. If instead we consider the differentiation with respect to the internal fermion mass m^2 rather than the bound state mass M^2, although it does not improve the wavefunction behavior at the endpoint $x = 0$, we can generate a model with both real and imaginary parts of the DVCS amplitudes. It is worthwhile to point out that in general the LFWFs for a hadron may be non-vanishing at the end points [21], and recent measurements of single spin asymmetries suggest that the GPDs are non-vanishing at $x = \zeta$ [22]. A more realistic estimate would require non-valence Fock states [23].

From the plots, we propose an optics analog of the behavior of the Fourier spectrum of the DVCS amplitude. In fact, the similarity of paraxial optics and quantum fields on the light cone was first explored long ago in [24,25]. In the case of DVCS, the final-state proton wavefunction is modified relative to the initial state proton wavefunction because of the momentum transferred to the quark in the hard Compton scattering. The quark momentum undergoes changes in both longitudinal (ζP^+) and transverse ($\Delta_\perp$) directions. We remind the reader that, to keep close contact with experimental analysis, we have kept $-t$ fixed while performing the Fourier transform over the ζ variable. Note that the integrals over x and ζ are of finite range. More importantly the upper limit of ζ integral is $\zeta_{\max}$ which in turn is determined by the value of $-t$. The finiteness of slit width is a *necessary* condition for the occurrence of diffraction pattern in optics. Thus when integration is performed over the range from 0 to $\zeta_{\max}$, this finite range acts as a slit of finite width and provides a necessary condition for the occurrence of diffraction pattern in the Fourier transform of the DVCS amplitude. When a diffraction pattern is produced, in analogy with single slit diffraction, we expect the position of the first minimum to be inversely proportional to $\zeta_{\max}$. Since $\zeta_{\max}$ increases with $-t$, we expect the position of the first minimum to move to a smaller value of σ, in analogy with optical diffraction. In the case of the Fourier spectrum of DVCS on the quantum fluctuations of a lepton target in QED, and also in the corresponding hadronic model, one sees that the diffractive patterns in σ sharpen and the positions of the first minima typically move in with increasing momentum transfer. Thus the invariant longitudinal size of the parton distribution becomes longer and the shape of the conjugate light-cone momentum distribution becomes narrower with increasing $|t|$. Regarding the diffraction patterns observed in the Fourier spectrum of the DVCS amplitude, we further note that for fixed $-t$, higher minima appear at positions which are integral multiples of the lowest minimum. This further supports the analogy with diffraction in optics.

We can study the diffraction pattern in σ as a function of t or $\Delta_\perp^2$ in order to register the effect of a change in transverse momentum resulting from the Compton scattering. If one Fourier transforms in ζ at fixed $\Delta_\perp$ and then Fourier transforms the change in transverse momentum $\Delta_\perp$ to impact space $b_\perp$ [4,5], then one would have the analog of a three-dimensional scattering center. In this sense, scattering photons in DVCS provides the complete Lorentz-invariant light front coordinate space structure of a hadron.

Acknowledgements

This work was supported, in part, by the US Department of Energy grant Nos. DE-AC02-76SF00515, DE-FG02-97ER-41029, and DE-FG02-87ER40371 and at the University of California, Lawrence Livermore National Laboratory under contract No. W-7405-Eng-48. This work was also supported in part by the Indo-US Collaboration project jointly funded by the US National Science Foundation (NSF) (INT0137066) and the Department of Science and Technology, India (DST/INT/US (NSF-RP075)/2001).

References

[1] S.J. Brodsky, M. Diehl, D.S. Hwang, Nucl. Phys. B 596 (2001) 99.
[2] M. Diehl, T. Feldmann, R. Jakob, P. Kroll, Nucl. Phys. B 596 (2001) 33; M. Diehl, T. Feldmann, R. Jakob, P. Kroll, Nucl. Phys. B 605 (2001) 647, Erratum.
[3] X.D. Ji, Phys. Rev. Lett. 78 (1997) 610, hep-ph/9603249.
[4] M. Burkardt, Int. J. Mod. Phys. A 18 (2003) 173.
[5] M. Burkardt, Phys. Rev. D 62 (2000) 071503; M. Burkardt, Phys. Rev. D 66 (2002) 119903, Erratum; J.P. Ralston, B. Pire, Phys. Rev. D 66 (2002) 111501.
[6] D.E. Soper, Phys. Rev. D 15 (1977) 1141.
[7] X. Ji, Phys. Rev. Lett. 91 (2003) 062001; A.V. Belitsky, X. Ji, F. Yuan, Phys. Rev. D 69 (2004) 074014.
[8] For a review, see S.J. Brodsky, H.C. Pauli, S.S. Pinsky, Phys. Rep. 301 (1998) 299, hep-ph/9705477.
[9] K. Hornbostel, S.J. Brodsky, H.C. Pauli, Phys. Rev. D 41 (1990) 3814.
[10] S.J. Brodsky, G.F. de Teramond, Phys. Rev. Lett. 96 (2006) 201601.
[11] D. Chakrabarti, A. Harindranath, J.P. Vary, Phys. Rev. D 71 (2005) 125012; D. Chakrabarti, A. Harindranath, L. Martinovic, G.B. Pivovarov, J.P. Vary, Phys. Lett. B 617 (2005) 92; D. Chakrabarti, A. Harindranath, L. Martinovic, J.P. Vary, Phys. Lett. B 582 (2004) 196.
[12] S.J. Brodsky, S.D. Drell, Phys. Rev. D 22 (1980) 2236.
[13] A. Harindranath, R. Kundu, A. Mukherjee, J.P. Vary, Phys. Rev. D 58 (1998) 114022; A. Harindranath, R. Kundu, Phys. Rev. D 59 (1999) 116013; A. Harindranath, R. Kundu, W.M. Zhang, Phys. Rev. D 59 (1999) 094013; A. Mukherjee, D. Chakrabarti, Phys. Lett. B 506 (2001) 283; A. Harindranath, A. Mukherjee, R. Ratabole, Phys. Lett. B 476 (2000) 471; A. Harindranath, A. Mukherjee, R. Ratabole, Phys. Rev. D 63 (2001) 045006.
[14] D. Chakrabarti, A. Mukherjee, Phys. Rev. D 71 (2005) 014038; D. Chakrabarti, A. Mukherjee, Phys. Rev. D 72 (2005) 034013.
[15] A. Mukherjee, M. Vanderhaeghen, Phys. Rev. D 67 (2003) 085020; A. Mukherjee, M. Vanderhaeghen, Phys. Lett. B 542 (2002) 245.
[16] S.J. Brodsky, D. Chakrabarti, A. Harindranath, A. Mukherjee, J.P. Vary, in preparation.
[17] S.J. Brodsky, D.S. Hwang, B.-Q. Ma, I. Schmidt, Nucl. Phys. B 593 (2001) 311.
[18] S.J. Brodsky, D.S. Hwang, I. Schmidt, Phys. Lett. B 530 (2002) 99, hep-ph/0201296.
[19] S.J. Brodsky, F.E. Close, J.F. Gunion, Phys. Rev. D 5 (1972) 1384; S.J. Brodsky, F.E. Close, J.F. Gunion, Phys. Rev. D 6 (1972) 177; S.J. Brodsky, F.E. Close, J.F. Gunion, Phys. Rev. D 8 (1972) 3678.
[20] P. Kroll, M. Schurmann, P.A. Guichon, Nucl. Phys. A 598 (1998) 435; M. Diehl, T. Gousset, B. Pire, J.P. Ralston, Phys. Lett. B 411 (1997) 193; A.V. Belitsky, D. Muller, L. Niedermeier, A. Schafer, Phys. Lett. B 474 (2000) 163.
[21] F. Antonuccio, S.J. Brodsky, S. Dalley, Phys. Lett. B 412 (1997) 104.
[22] A. Airapetian, et al., HERMES Collaboration, Phys. Rev. Lett. 87 (2001) 182001; S. Stepanyan, et al., CLAS Collaboration, Phys. Rev. Lett. 87 (2001) 182002.
[23] C.R. Ji, Y. Mishchenko, A. Radyushkin, hep-ph/0603198.
[24] E.C.G. Sudarshan, R. Simon, N. Mukunda, Phys. Rev. A 28 (1983) 2921, DOE-ER-03992-503.
[25] N. Mukunda, R. Simon, E.C.G. Sudarshan, Phys. Rev. A 28 (1983) 2933, DOE-ER-03992-504.